Environment International 136 (2020) 105425

Contents lists available at ScienceDirect

Environment International

journal homepage: www.elsevier.com/locate/envint

Temperature-dependent luminescence spectroscopic and mass spectrometric investigations of U(VI) complexation with aqueous silicates in the acidic pH-range

Henry Lösch[a], Manuel Raiwa[b], Norbert Jordan[a], Michael Steppert[b], Robin Steudtner[a], Thorsten Stumpf[a], Nina Huittinen[a,*]

[a] Helmholtz–Zentrum Dresden–Rossendorf, Institute of Resource Ecology, Bautzner Landstraße 400, 01328 Dresden, Germany
[b] Institute of Radioecology and Radiation Protection, Leibniz Universität Hannover, Herrenhäuser Straße 2, 30419 Hannover, Germany

ARTICLE INFO

Handling Editor: Thanh Nguyen

Keywords:
Luminescence
Silicates
Uranium(VI)
Complexation
Thermodynamic constants
Temperature dependent

ABSTRACT

In this study the complexation of U(VI) with orthosilicic acid (H_4SiO_4) was investigated between pH 3.5 and 5 by combining electrospray ionization mass spectrometry (ESI-MS) and laser-induced luminescence spectroscopy. The ESI-MS experiments performed at a total silicon concentration of $5 \cdot 10^{-3}$ M (exceeding the solubility of amorphous silica at both pH-values) revealed the formation of oligomeric sodium-silicates in addition to the $UO_2OSi(OH)_3^+$ species. For the luminescence spectroscopic experiments (25 °C), the U(VI) concentration was fixed at $5 \cdot 10^{-6}$ M, the silicon concentration was varied between $1.3 \cdot 10^{-4}$–$1.3 \cdot 10^{-3}$ M (reducing the formation of silicon oligomers) and the ionic strength was kept constant at 0.2 M $NaClO_4$. The results confirmed the formation of the aqueous $UO_2OSi(OH)_3^+$ complex. The conditional complexation constant at 25 °C, log $^*\beta = -(0.31 \pm 0.24)$, was extrapolated to infinite dilution using the Davies equation, which led to log $^*\beta^0 = -(0.06 \pm 0.24)$. Further experiments at different temperatures (1–25 °C) allowed the calculation of the molal enthalpy of reaction $\Delta_r H_m^0 = 45.8 \pm 22.5$ kJ·mol^{-1} and molal entropy of reaction $\Delta_r S_m^0 = 152.5 \pm 78.8$ J·K^{-1}·mol^{-1} using the integrated van't Hoff equation, corroborating an endothermic and entropy driven complexation process.

1. Introduction

Uranium is a common radioactive contaminant in our environment, originating from various mining and milling activities, from the reprocessing of spent nuclear fuel, and from other processes related to nuclear energy or weapons production (Choppin et al., 2013; Grenthe et al., 2006). In addition, uranium is the main constituent in spent nuclear fuel (SNF), which, in many countries, will be disposed of as such in underground waste repositories (Hedin, 1997; Bruno and Ewing, 2006; OECD/NEA, 2006; Brasser et al., 2008; Kim et al., 2011). The main transport path for uranium in the (sub)surface environment is the migration with groundwater where the uranium speciation will be governed by the groundwater parameters such as the temperature, pH, redox potential (E_h), and the chemical composition in terms of dissolved inorganic and organic species (Gibb, 1999; Myllykylae, 2008–2009; Altmaier and Vercouter, 2012; Maher et al., 2012). Thus, for the prediction of the uranium mobility in the environment, reliable thermodynamic data such as complexation constants, solubility products, reaction enthalpies and entropies for various inorganic and organic uranium complexes are required.

Due to the ubiquitous presence of silicon in the environment, various monomeric, polymeric or colloidal silicate species may influence the uranium speciation in the groundwater. In future nuclear waste repositories containing vitrified waste, the dissolution process of borosilicate glass mold produced in the reprocessing of SNF could be an additional silicon source depending on the conditions in the repository (Grambow, 2006). Monomeric species, such as orthosilicic acid H_4SiO_4 and its deprotonated form $H_3SiO_4^-$ are known to prevail at pH-values below 9. At pH > 9, increasing amounts of $H_2SiO_4^{2-}$ and various polymeric silicates are formed in solution, resulting in an increased overall silicate solubility (Sjöberg, 1996). In the acidic to neutral pH-range the solubility limit of amorphous silica is approximately $2 \cdot 10^{-3}$ M (Siever, 1957; Marshall, 1980; Marshall and Warakomski, 1980; Reiller et al., 2012).

Due to the complexity of Si polymeric species, very little is known in general about metal ion complexation with these polymers. In the case

* Corresponding author.
E-mail address: n.huittinen@hzdr.de (N. Huittinen).

https://doi.org/10.1016/j.envint.2019.105425
Received 10 September 2019; Received in revised form 13 December 2019; Accepted 13 December 2019
Available online 31 January 2020

Table 1
Summary of the An(VI) complexation studies with aqueous silicates at 25 °C.

Method	Formed complex	pH-range	I (M)	[Si] (M)	[An] (M)	log $*\beta^0$	Ref.
lumin. spec.	$UO_2OSi(OH)_3^+$	3.5	0.2	$1.3 \cdot 10^{-4}$–$1.3 \cdot 10^{-3}$	$5 \cdot 10^{-6}$	−(0.06 ± 0.24)	p.w.
TRLFS	$UO_2OSi(OH)_3^+$	3.9	0.3	$1.6 \cdot 10^{-4}$–$5.4 \cdot 10^{-3}$	$2.3 \cdot 10^{-5}$	−(1.44 ± 0.20)	(Moll et al., 1998)
solv. extr.	$UO_2OSi(OH)_3^+$	3–4.5	0.2	1.7–$6.7 \cdot 10^{-2}$	^{233}U trace	−(1.74 ± 0.09)	(Satoh and Choppin, 1992)
spectrophoto.	$UO_2OSi(OH)_3^+$	2.5–5.1	0.1	0–$1.7 \cdot 10^{-3}$	$1 \cdot 10^{-5}$	−(2.65 ± 0.06)	(Jensen and Choppin, 1998)
spectrophoto.	$UO_2OSi(OH)_3^+$	~3.7	0.2	2.4–$3.5 \cdot 10^{-2}$	$6.4 \cdot 10^{-4}$	−(1.71 ± 0.13)	(Porter and Weber, 1971)
solv. extr.	$UO_2OSi(OH)_3^+$	3.3–4.5	0.2	1.0–$6.7 \cdot 10^{-2}$	^{232}U trace	−(1.94 ± 0.06)	(Hrnecek and Irlweck, 1999)
solv. extr.	$UO_2OSi(OH)_3^+$	3.6	0.2	0–$1.2 \cdot 10^{-3}$	^{233}U trace	−(2.39 ± 0.04)	(Pathak and Choppin, 2006)
spectrophoto.	$UO_2OSi(OH)_3^+$	1.7–4.25	0.2	1.0–$8.0 \cdot 10^{-3}$	$3 \cdot 10^{-4}$–$7 \cdot 10^{-3}$	−(2.29 ± 0.04)	(Yusov and Fedoseev, 2005)
TRLFS	$UO_2OSi(OH)_3^+$	4	0.1	$1.0 \cdot 10^{-6}$ – $3.2 \cdot 10^{-3}$	$2.5–10^{-5}$	−(0.72 ± 0.20)	(Saito et al., 2015)
spectrophoto.	$NpO_2OSi(OH)_3^+$	1.7–4.7	0.2	2.2–$8.8 \cdot 10^{-2}$	$6 \cdot 10^{-4}$–$3.2 \cdot 10^{-3}$	−(2.61 ± 0.12)	(Yusov et al., 2005)
spectrophoto.	$PuO_2OSi(OH)_3^+$	4.25–6.5	0.2	$5.0 \cdot 10^{-3}$–$2.5 \cdot 10^{-2}$	$2.5 \cdot 10^{-5}$–$7 \cdot 10^{-4}$	−(3.64 ± 0.17)	(Yusov and Fedoseev, 2003)

of orthosilicic acid, several studies exist where the complexation of U (VI), which is the prevailing oxidation state of uranium under oxic conditions, with the $H_3SiO_4^-$ ligand has been investigated (Table 1). The complexation constants for the $UO_2OSi(OH)_3^+$ complex have been determined with different experimental methods such as solvent extraction (Satoh and Choppin, 1992; Hrnecek and Irlweck, 1999; Pathak and Choppin, 2006), spectrophotometry (Porter and Weber, 1971; Jensen and Choppin, 1998; Yusov and Fedoseev, 2005), and time-resolved laser-induced luminescence spectroscopy (TRLFS) (Moll et al., 1998; Saito et al., 2015). The magnitude of the complexation constant, however, is varying by almost two orders of magnitude depending on the study. When including complexation constants for the analogous silicate complex with other hexavalent actinides ($NpO_2OSi(OH)_3^+$ and $PuO_2OSi(OH)_3^+$) in the comparison, the discrepancy between the largest reported value −(0.91 ± 0.20) (Saito et al., 2015) and the lowest one −(3.64 ± 0.17) (Yusov and Fedoseev, 2003), is almost three orders of magnitude (Table 1). This discrepancy may arise from the use of rather high total silicon concentrations (above the solubility limit of amorphous silica, 2 mM) in some of the studies, which can lead to the formation of polysilicates or colloidal silica. In addition, a recent study showed that U(VI) hydrolysis has to be considered when studying uranyl(VI) complexation reactions with silicates at a mildly acidic pH value of 4.0 (Saito et al., 2015). When such hydrolysis reactions are not considered, the obtained complexation constants are typically too low, as the free UO_2^{2+} concentration in solution is overestimated.

Thus, to understand the effects of aqueous uranium hydroxo and polysilicate species on the U(VI)-silicate complexation, we investigated the complexation of UO_2^{2+} with dissolved silicates at under- and oversaturation conditions (with respect to amorphous silica) using a combination of Electrospray-Ionization Mass spectrometry (ESI-MS) and laser-induced luminescence spectroscopy as experimental methods. ESI-MS is a well suited technique to investigate the solution chemistry in inorganic as well as organic solutions as it delivers intrinsic information of the formed species such as their mass-to-charge ratios and their stoichiometries (Moulin et al., 2000; Moulin, 2003; Zubarev and Makarov, 2013). Laser-induced luminescence spectroscopy allows the *in situ* monitoring of complexation reactions with U(VI) in aqueous environments down to concentrations of 10^{-9} M (Moulin et al., 1998; Drobot et al., 2016), as well as the identification of the prevailing species and their stochiometries. Silicate solutions in the absence and presence of UO_2^{2+} were analyzed by ESI-MS to investigate the presence of monomeric and/or polymeric silicates in solution and the formation of U(VI)-silicate complexes. As environmental conditions comprise temperatures above and below 25 °C, the luminescence spectroscopic investigations have been conducted in the temperature range from 1 to 25 °C to enable the derivation of temperature-dependent complexation constants for the $UO_2OSi(OH)_3^+$ complex as well as thermodynamic data, i.e. the molal enthalpy of reaction $\Delta_rH_m^0$ and molal entropy of reaction $\Delta_rS_m^0$. Temperatures above 25 °C were not investigated, to avoid dealing with the formation of colloidal silicate species.

2. Materials and methods

2.1. Sample preparation

All solutions were prepared with high purity reagent grade materials without further treatment. For the ESI-MS samples the U(VI) concentrations were $1 \cdot 10^{-5}$ and $1 \cdot 10^{-4}$ M, and the silicate concentration ranged between $1 \cdot 10^{-3}$ and $5 \cdot 10^{-3}$ M. For the silicon stock-solution, sodium-metasilicate (J.T. Baker) was dissolved in Milli-Q water and the pH was adjusted to 3.5 or 5.0 with 1 M $HClO_4$ and 1 M NaOH. No further ionic strength adjustments were performed to avoid salt crystal formation in the ESI-MS needle and to reduce artefacts during the ESI-MS measurements.

For the luminescence spectroscopic investigations a $U(VI)_{nat}$-stock solution with a concentration of $1 \cdot 10^{-4}$ M in 1 M $HClO_4$ (Merck-Emsure) was used for all experiments. As a silicon source, a Si-ICP standard in NaOH (Sigma-Aldrich, TraceCERT) with a concentration of 1000 mg·L^{-1} was diluted in 0.235 M $NaClO_4$ (VWR Chemicals) to obtain a Si-stock solution with a concentration of $5 \cdot 10^{-3}$ M which was immediately used for the preparation of the U(VI)-silicate samples. Aliquots of the U(VI) and Si-stock solutions were mixed in 0.2 M $NaClO_4$ to reach final concentrations of $5 \cdot 10^{-6}$ M and $1.3 \cdot 10^{-4} – 1.3 \cdot 10^{-3}$ M, respectively, in the samples. The pH was adjusted to 3.5 with 1 M $HClO_4$ and 1 M NaOH (Carl Roth). To avoid chloride impurities in the samples which cause severe quenching of the U(VI) luminescence signal (Yokoyama et al., 1976; Burrows, 1990; Tsushima et al., 2010; Haubitz et al., 2018), a double junction electrode (Metrohm, EtOH-Trode) filled with 0.2 M $NaClO_4$ was used for pH adjustments. The absence of colloidal species was checked in all samples by means of ultracentrifugation, dynamic light scattering, and the molybdate-method (further description is given in the SI).

2.2. ESI-MS

The experiments were performed with a Velos Pro Orbitrap Elite (Thermo Fisher Scientific Inc.) using a Nanospray Flex Source. Ten microliter of the sample solution was loaded into GlassTip™ Emitters from New Objective Inc. (Woburn) and analyzed with the Orbitrap mass analyzer. Full-MS scans with *m/z* ranging from 200 to 2000 were recorded and averaged for at least three minutes. Ions with a lower *m/z* value were measured independently with scans at *m/z* from 100 to 200 and *m/z* from 50 to 100. This is necessary as ions in this low range require a change of the applied radio frequency voltages of the ion transfer optics, resulting in a loss of ions with a high *m/z* value. This unfortunately results in a loss of comparability of the relative intensities of the different species between these regions. A comparison of the relative intensities within the *m/z* region is still possible, however. Mass accuracy around 1 ppm was ensured with known lock masses from ambient air. The temperature of the transfer capillary was fixed at 240 °C.

Eight U-Si samples were measured in the positive ion mode with a

voltage of 1.8 kV applied to the nanospray emitter, whereas four Si-stock solutions without U(VI) were analysed in the negative ion mode with an applied voltage of 1.8 kV. The data treatment was done with the Xcalibur and Freestyle software from Thermo Fisher.

2.3. Laser-induced luminescence spectroscopy

The complexation reaction of U(VI) with aqueous silicates was investigated with luminescence spectroscopy from 3 mL sample in quartz glass cuvettes. The U(VI) was excited in the absorption maximum at λ_{ex} = 266 nm with a Minilite laser system (Continuum) with an energy of 0.3 mJ. The light was guided into an iHR550 spectrograph (Horiba Scientific) with an entrance slit of 200 μm and a spectral grating of 150 lines · mm^{-1}. The spectra were recorded with an ICCD camera (Horiba Scientific), 0.1 μs after the laser pulse with a gate width of 500 μs. For the temperature dependent measurements, the cuvette housing was equipped with a Peltier-element for equilibration and measurement of the samples at the desired temperatures between 1 and 25 °C.

2.4. Speciation calculations

To predict the concentration of H_4SiO_4 in the solutions at varying temperatures (1–25 °C), the silicate speciation was calculated with PhreeqC (Parkhurst and Appelo, 1999). The ThermoChimie database (version 9b0, Giffaut et al., 2014) from ANDRA using the Davies equation for the treatment of the activity coefficients was used. The calculations were performed at a fixed ionic strength of 0.2 M $NaClO_4$, at pH = 3.5. The total silicic acid concentration ranged from $1.3 \cdot 10^{-4}$ to $1.3 \cdot 10^{-3}$ M, according to the luminescence spectroscopic investigations.

3. Results

3.1. ESI-MS investigations

For the determination of the silicate speciation in solution in the absence and presence of U(VI), mass spectrometric investigations were conducted at under- and oversaturation conditions (i.e. below and above $2 \cdot 10^{-3}$ M) of the solubility of amorphous silica (Fig. SI 1) for two different pH-values of 3.5 and 5.0. This pH-range was chosen to cover the majority of experimental conditions used in previous U(VI)-silicate studies, see Table 1. Blank solutions without silicates consisting of $1 \cdot 10^{-5}$ M UO_2^{2+} at pH 3.5 and 5.0 were also measured to identify the solution signals, which do not arise from silicate species. The MS spectra of these blank solutions are presented in the supplementary information (Fig. SI 2). At pH 5.0 (Fig. SI 2, left) the spectrum is dominated by signals from $[Na(NaClO_4)]_n^+$ chains (n = 1–9) associated with different quantities of H_2O. This chain formation has already been observed in previous studies (Moulin et al., 2000; Schröder, 2012). The signals consist of characteristic clustered peaks with a consistent *m/z* gap arising from the presence of two chlorine isotopes ^{35}Cl and ^{37}Cl with abundances of 75.76% and 24.24%, respectively. At pH 3.5 the chains are also visible but less pronounced (Fig. SI 2, right). Thus, for the sake of clarity, all signals related to the background, i.e. $NaClO_4$ as well as signals arising from room air have been plotted in gray in the following figures.

In addition to the aforementioned background signals, both blank solutions show signals for the free uranyl(V) UO_2^+ cation (*m/z* 270.04) and the 1:1 hydroxo UO_2OH^+ species with different quantities of H_2O (*m/z* 287.04, 305.05, and 323.06) (Fig. 1 bottom left, black traces, Table 2). Especially the UO_2^{2+} cation is prone to collision induced reduction in the gas phase according to Eq. (1).

$$UO_2^{2+} + X \rightleftharpoons UO_2^+ + X^+ \quad (1)$$

In other words, the presence of U(V) species in the ESI-MS spectra is merely an artefact arising from UO_2^{2+} and not a real species in the original U-containing solutions. Furthermore, three additional signals at *m/z* 365.02, 383.03, and 401.04 were identified in the mass spectra (Fig. 1 bottom left, red traces). As the tip of the ESI needle is made of glass, these signals are related to U-Si-species ($UO_2OSi(OH)_3^+ \pm H_2O$) produced at the needle tip. At higher *m/z* ratios no additional signals were identified. Thus, for a positive identification of formed U-Si species in the silicon-containing solutions, this background signal has to be accounted for. In the Orbitrap the ions are collected in different traps and additionally collision-cooled with nitrogen to remove the solvation shell around the ions and to minimize energy distribution before the *m/z* analysis. The removal of the solvation shell and the collision-cooling might lead to fragmentation of polynuclear U-hydroxo species. Therefore, the concentration of the 1:1 hydroxo species could be overestimated in the MS-spectra in comparison to the original concentration in solution.

Following the investigations of pure U(VI) solutions, two silicate-containing solutions with an overall silicate concentration of $1 \cdot 10^{-3}$ M were investigated in the absence of uranium(VI) at pH 3.5 and 5.0 in the anion mode (negative mode). Even though the silicate concentration in the solutions is lower than the solubility limit for amorphous silica, both solutions show the presence of oligomeric Si- and Na-Si-species in the mass spectra at *m/z* 70–500 (Figs. SI 3 and SI 4). The relative concentration of these oligomers is up to five times larger at pH 5.0 than at pH 3.5 based on the relative intensities (Fig. SI 4). In the lower *m/z*-ratio (50–100 and 130–160) the signals of the monomeric and dimeric species were also visible (Fig. SI 3). As already mentioned the comparison between the different *m/z* is not possible due to different sensitivity in these regions. The $Si_3O_9H_4Na^-$ complex is the dominant species in the high *m/z*-region. Based on the chemical formula a triangular or linear structure of the molecule is possible. The observed signals are summarized in Table SI 1. The assignment of the Si- and Na-Si-species follows the work of Pelster et al. (2006).

In undersaturated silicate solutions [Si] = $1 \cdot 10^{-3}$ M at pH 3.5 with [U(VI)] = $1 \cdot 10^{-5}$ M an increase of the relative intensity of the $UO_2OSi(OH)_3^+$ signals as well as a decrease of the U-hydroxo related signals in comparison to the blank solution was observed (Fig. 1 top left, red traces).

Furthermore, new signals appear at *m/z* 274.93, 334.89, and 352.90 as well as in the *m/z* range between 410 and 800 at *m/z* 442.99, 461.00, 479.01, and 430.89 + n · (*m/z* = 59.97) with n = 0–5 (Fig. 1 top right). These signals stem from oligomeric Na-Si-species with up to 10 silicon units as well as U-Si-species with three silicon units in solution, see Table 2.

A comparison of the relative intensities (after subtraction of the background signals) reveals that the amount of monomeric species in solution is 23 times higher than the polymeric U-Si species at pH 3.5. An increase of the pH to 5.0 decreases the ratio to 16, implying that a greater amount of polymers are forming at this pH-value. When increasing the silicate concentration in solution to $5 \cdot 10^{-3}$ M, i.e. above the solubility limit of amorphous silica, the signals at *m/z* 430.89 + n (*m/z* = 59.97) with n = 0–5 get more pronounced (Fig. SI 6 in SI). By simultaneously increasing the uranium concentration to $1 \cdot 10^{-4}$ M, the oversaturated solution shows the presence of additional signals in the *m/z* range of 410–800 at 520.97, 616.96, 694.94, and 790.69 (Fig. SI 7 in SI). The assignment of the signals reveal the existence of U-Si-species up to four silicon units and Na-Si-species up to 11 silicon units in solution (Table 2, Table SI 1, Table Si 2). Eventually, the increase of the solution pH at [U(VI)] = $1 \cdot 10^{-5}$ M and [Si] = $1 \cdot 10^{-3}$ M, showed a similar increase of the polymeric uranium-silicate species as observed at lower pH, but at oversaturation conditions (Fig. SI 5 in SI). Thus, the results of the mass spectrometric investigations can be summarized as follows: the monomeric U(VI)-silicate ($UO_2OSi(OH)_3^+$) species dominates the solution speciation at pH 3.5 at undersaturation conditions with minor amounts of polymeric species. Upon increasing the pH, a

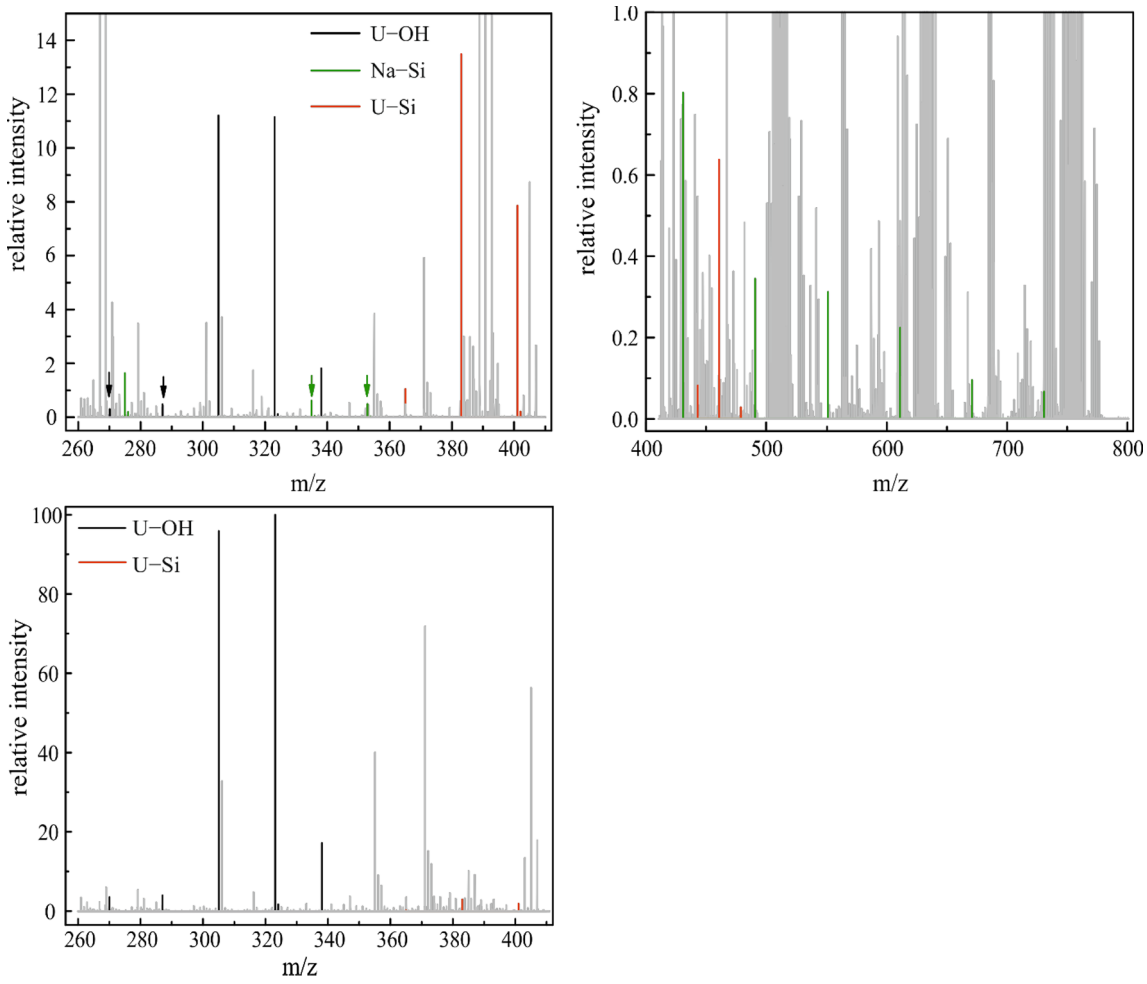

Fig. 1. MS-spectra of an uranyl(VI) silicate solution at pH 3.5 with [U(VI)] = $1 \cdot 10^{-5}$ M, [Si] = $1 \cdot 10^{-3}$ M, top left *m/z* 260–410 (arrows for better visibility), top right: *m/z* 400–800 (positive mode), bottom left: MS-spectra of an uranyl(VI) reference solution in absence of silicate at pH 3.5 with the same conditions (positive mode). The abbreviation U-OH in the figures stand for free uranyl(VI) and uranyl(VI)-hydroxo species.

greater U-concentration and/or a higher silicate concentration enhances the formation of oligomeric U-silicates. For example, by increasing the silicate concentration from $1 \cdot 10^{-3}$ M to mild oversaturation concentrations of $5 \cdot 10^{-3}$ M at pH = 5.0 leads to a change of ratio of the relative intensities of monomeric to polymeric species from 16 to 5. The exact structures of these Si-polymers cannot

Table 2
Assigned U-OH, U-Si and Na-Si species (rel. I - relative intensities) in aqueous uranyl(VI)-silicate solutions and their relative intensities at pH 3.5 (see Fig. 1) and at pH 5.0 (see Fig. SI 5) with [U(VI)] = $1 \cdot 10^{-5}$ M, [Si] = $1 \cdot 10^{-3}$ M and U-reference solutions [U(VI)] = $1 \cdot 10^{-5}$ M in absence of aqueous silicates at 25 °C (positive mode).

m/z	Species	pH 3.5 [Si] = $1 \cdot 10^{-3}$ in M rel. I	pH 5.0 [Si] = $1 \cdot 10^{-3}$ in M rel. I	pH 3.5 [Si] = 0 in M rel. I	pH 5.0 [Si] = 0 in M rel. I
270.04	UO_2^+	0.30	0.67	3.49	2.49
274.93	$Si_3O_{10}H_8Na^+$	1.63	1.86	–	–
287.04	UO_2OH^+	0.47	0.58	3.93	3.90
305.05	$UO_2OH^+ + H_2O$	11.21	14.24	95.92	96.02
323.06	$UO_2OH^+ + 2H_2O$	11.14	14.67	100	100
334.89	$Si_4O_{12}H_8Na^+$	0.61	0.77	–	–
352.90	$Si_4O_{13}H_{10}Na^+$	0.49	0.54	–	–
365.05	$UO_2OSi(OH)_3^+$	1.04	2.10	0.17	0.42
383.03	$UO_2OSi(OH)_3^+ + H_2O$	13.48	28.56	2.97	8.19
401.04	$UO_2OSi(OH)_3^+ + 2H_2O$	7.86	17.67	1.85	4.95
430.89	$Si_5O_{16}H_{12}Na^+$	0.8	1.12	–	–
442.99	$UO_2OSi(OH)_3OSi(OH)_2^+$	0.08	0.38	–	–
461.00	$UO_2OSi(OH)_3OSi(OH)_2^+ + H_2O$	0.64	1.50	–	–
479.01	$UO_2OSi(OH)_3OSi(OH)_2^+ + 2H_2O$	0.03	0.22	–	–
490.85	$Si_6O_{18}H_{12}Na^+$	0.34	0.48	–	–
550.82	$Si_7O_{20}H_{12}Na^+$	0.31	0.48	–	–
610.79	$Si_8O_{22}H_{12}Na^+$	0.22	0.41	–	–
670.75	$Si_9O_{24}H_{12}Na^+$	0.1	0.31	–	–
730.72	$Si_{10}O_{26}H_{12}Na^+$	0.08	0.25	–	–

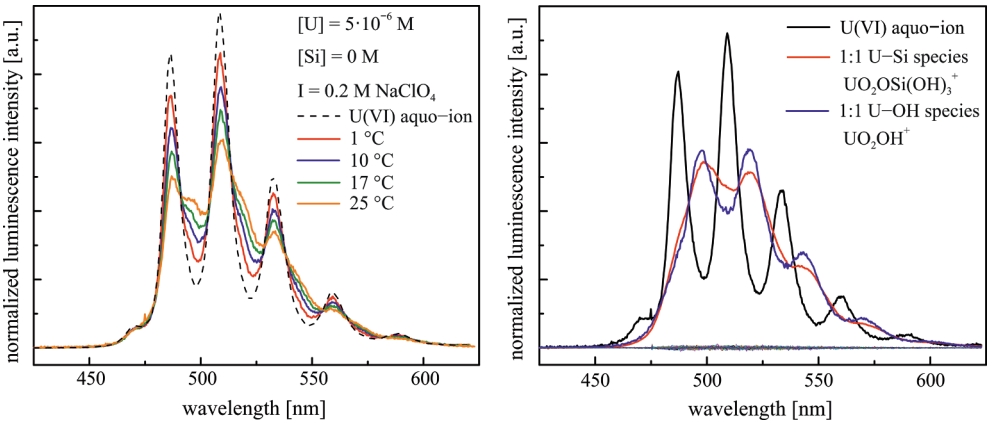

Fig. 2. Left: Emission spectra of the U(VI) solution in the absence of aqueous silicates at pH 3.5, [U(VI)] = $5 \cdot 10^{-6}$ M in 0.2 M $NaClO_4$ at different temperatures (normalized to area under peak). Dashed line: free U(VI) aquo-ion [U(VI)] = $5 \cdot 10^{-6}$ M in 0.2 M $NaClO_4$ at pH 1, 25 °C. right: Extracted free component spectra from recorded emission spectra collected in silicate-containing solutions corresponding to the free UO_2^{2+} aquo-ion (—), the 1:1 UO_2OH^+ hydroxo complex (—) and the $UO_2OSi(OH)_3^+$ complex (—) with residuals (normalized to area under peak).

be assigned based on their MS-spectra as already concluded by Pelster et al. (2006). For the derivation of complexation constants and thermodynamic data for the $UO_2OSi(OH)_3^+$ complex (see next section), the experimental conditions were limited to the lower pH of 3.5, using an overall uranium(VI) concentration of $5 \cdot 10^{-6}$ M and a total silicate concentration below the solubility limit, in the range from $1.3 \cdot 10^{-4}$ to $1.3 \cdot 10^{-3}$ M, in order to suppress the formation of polymeric U-Si and Si-species in solution.

3.2. Luminescence spectroscopic investigations

The recorded U(VI) luminescence emission spectra at pH 3.5 and temperatures between 1 and 25 °C in the absence of aqueous silicates show the presence of two different U-species (Fig. 2, left). At 1 °C, the spectra resemble that of the pure UO_2^{2+} aquo-ion (dashed traces). However, with increasing temperature from 1 to 25 °C, clear shoulders start appearing between the main peaks of the aquo-ion, as a result of increasing U(VI) hydrolysis. To obtain the pure component spectra of the individual species a peak deconvolution was performed based on a non-linear least squares fit method. As every species has a different quantum efficiency relative to the free uranyl(VI) aquo ion, a correction factor for each species has to be taken into account to calculate the corrected species distribution. These correction factors (luminescence intensity factors - LI, see Table 3) were determined relative to the uranyl(VI) aquo-ion (relative intensity = 1). A non-linear least squares fit method was used to derive the LI factors, followed by correction of the species distribution using these factors. A comprehensive discussion of the deconvolution process and the calculation of the luminescence intensity factors can be found in Huittinen et al. (2012) and Fanghänel et al. (1998). The single component spectrum extracted by spectral deconvolution from the measured data, is consistent with the published spectrum of the 1:1 U-hydroxo species UO_2OH^+ (Fig. 2, right black traces) (Drobot et al., 2016). Also Moulin et al. (1995) showed a contribution of the first U-hydroxo species in the emission spectra at pH 3.5 next to the free aquo-ion. This implies that U-hydrolysis plays a role in the U(VI) speciation already at this low pH and it has to be considered in the U(VI)-silicate complexation investigations, in agreement with the results published in Saito et al. (2015).

With increasing silicate concentration a change in the spectral shape combined with a continuous red-shift of the measured spectra can be seen in addition to a slight increase of the luminescence intensity (Fig. 3, left and Fig. SI 8 in SI). As the relative amount of polymeric silicate species at these conditions were found to be negligible in our mass spectrometric investigations, these changes can, thus, be attributed to the complexation reaction between U(VI) and aqueous monosilicates. As shown in Fig. 2 (left), increasing temperature leads to an increased formation of the uranium hydrolysis species. Next to the free UO_2^{2+} (Fig. 2, right black traces) and the 1:1 hydroxo species (Fig. 2, right, blue traces), an U-Si species could be extracted in the deconvolution process (Fig. 2, right red traces). The calculated species distribution at 25 °C is shown in Fig. 3 (right). The species distributions at the other investigated temperatures can be found in the SI (Fig. SI 9 in SI).

Table 3
Conditional (log *β, I = 0.2 M $NaClO_4$) (values are provided in the molal scale) and extrapolated to infinite dilution (log $*\beta^0$) complexation constant of the $UO_2OSi(OH)_3^+$ complex at different temperatures with the associated LI-factors.

Temp. (°C)	log *β(T)	log $*\beta^0$(T)	LI $UO_2OSi(OH)_3^+$	LI UO_2OH^+
1	−(1.01 ± 0.27)	−(0.76 ± 0.27)	2.82	0.64
10	−(0.74 ± 0.19)	−(0.49 ± 0.19)	3.08	0.72
17	−(0.53 ± 0.33)	−(0.28 ± 0.33)	4.42	1.17
25	−(0.31 ± 0.24)	−(0.06 ± 0.24)	6.81	1.78

3.3. Determination of the conditional constants at 25 °C

From the derived species distribution the molar concentration of the UO_2^{2+}, UO_2OH^+ and $UO_2OSi(OH)_3^+$ species were obtained and converted to the molal scale. For the conversion, the density of the background electrolyte $NaClO_4$ at the used concentration of 0.2 M and temperature of 25 °C was required and taken from Söhnel and Novotny (1985). The concentration of the orthosilicic acid at the used conditions was calculated using PhreeqC, the Thermochimie database (Version 9b0, Giffaut et al., 2014) and the Davies equation for calculating the activity coefficients of ions.

Since the concentration of U(VI) was orders of magnitude lower than that of the silicate species, we assumed that the silicate speciation was not significantly impacted by the complexation with U(VI). With the molalities of UO_2^{2+}, the formed complexes, and the orthosilicic acid, conditional complexation constant could be derived based on the following equilibrium:

$$UO_2^{2+} + H_4SiO_4 \rightleftharpoons UO_2OSi(OH)_3^+ + H^+ \quad (2)$$

By applying the law of mass action the following expression of the conditional complexation constant was obtained:

$$\log *\beta(I) = \log\left(\frac{m_{UO_2OSi(OH)_3^+} \cdot m_{H^+}}{m_{UO_2^{2+}} \cdot m_{H_4SiO_4}}\right) \quad (3)$$

The symbol * describes a reaction involving a deprotonation of the ligand as written in Eq. (2) (Lemire et al., 2013), and will be used further in the text. A re-arrangement of Eq. (3) allows the plot of $\log \frac{m_{UO_2OSi(OH)_3^+}}{m_{UO_2^{2+}}} + \log m_{H^+}$ as a function of $\log m_{H_4SiO_4}$ at an ionic strength of 0.2 M and temperatures ranging from 1 to 25 °C (Fig. 4).

For all investigated temperatures a slope close to one was obtained,

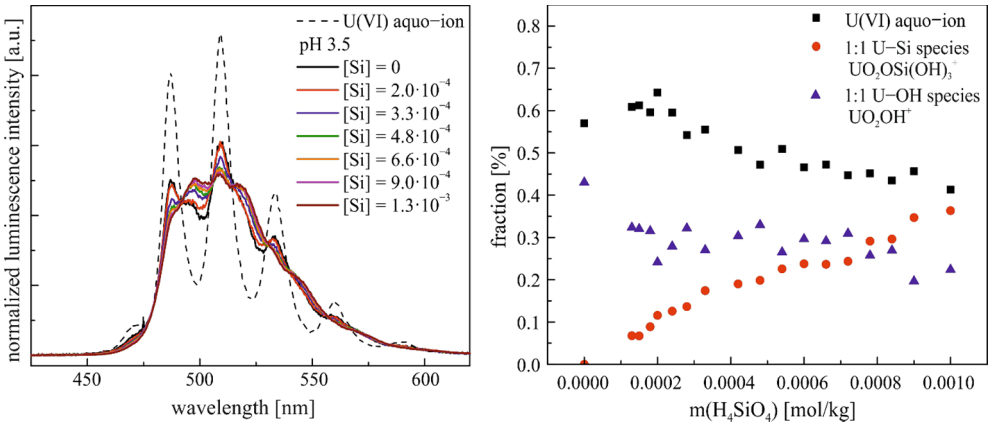

Fig. 3. Left: Emission spectra of aqueous uranium-silicate complexation [U(VI)] = $5 \cdot 10^{-6}$ M at pH 3.5 with increasing silicate concentration ($1.3 \cdot 10^{-4} - 1.3 \cdot 10^{-3}$ M) at 25 °C (normalized to area under peak). Dashed line: free U(VI) aquo-ion [U(VI)] = $5 \cdot 10^{-6}$ M in 0.2 M $NaClO_4$ at pH 1, 25 °C. right: Extracted species distribution at 25 °C in the presence of aqueous silicates.

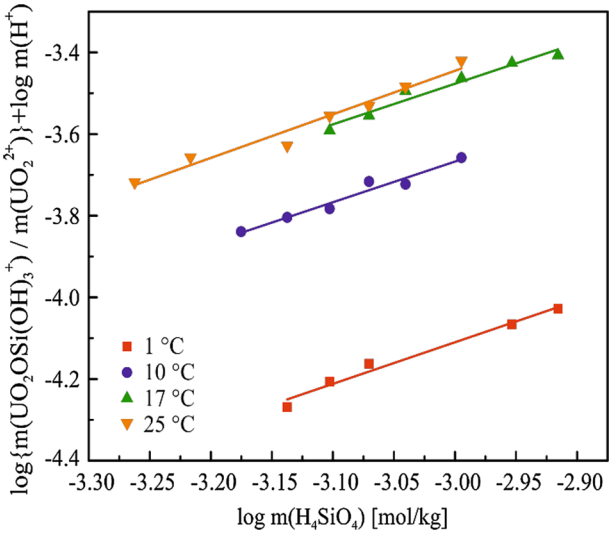

Fig. 4. Slope analysis of the complexation reaction $UO_2^{2+} + H_4SiO_4 \rightleftharpoons UO_2OSi(OH)_3^+ + H^+$ at different temperatures.

confirming the stoichiometry of the postulated $UO_2OSi(OH)_3^+$ complex. The intercept of the line with the y-axis corresponds to the conditional complexation constant. The temperature-dependent complexation constants at 0.2 M are compiled in Table 3.

To extrapolate the conditional constants to infinite dilution (log $*\beta^0$) the activity coefficients (γ_i) of the participating species need to be considered. These were calculated using the Davies equation (Eq. (4)), where A is the temperature dependent Debye-Hückel constant (Guillaumont et al., 2003), z_i, the charge of the ion, and I_m, the ionic strength in the molal scale.

$$log\gamma_i = -Az_i^2\left(\frac{\sqrt{I_m}}{1+\sqrt{I_m}} - 0.3I_m\right) \quad (4)$$

The uncertainty assigned to the value log $*\beta^0$ was taken identical to the experimental uncertainty. This extrapolation method was preferred to the specific ion interaction (SIT) theory, which requires the knowledge of the $\varepsilon(UO_2OSi(OH)_3^+;ClO_4^-)$ ion interaction coefficient. Even though the NEA TDB recommends the use of the SIT method, they do not provide an experimental value for this coefficient (Lemire et al., 2013). Only an estimated value of 0.30 is provided by the NEA without further information how this parameter was derived. One could have used a value of 0.20, as proposed by Thoenen et al. (2014) who were aiming at providing "default values" exclusively based on a charge consideration criterion. But this approximation does not consider size and electronic density distribution factors, which can lead to significant difference compared to experimentally determined ε values (see Jordan et al. (2018)), which can at the end severely impact the value of the extrapolated complexation constant at infinite dilution. Consequently, we applied the Davies equation, which should still be appropriate for the calculation of the activity coefficients up to 0.5 m ionic strengths (Bethke, 1996).

The Debye–Hückel constant A was taken from tabulated values (Lemire et al., 2013), at 10 °C (0.498 $kg^{1/2}$ $mol^{-1/2}$) and 25 °C (0.509 $kg^{1/2}$ $mol^{-1/2}$). Respective values at 1 °C (0.492 $kg^{1/2}$ $mol^{-1/2}$) and 17 °C (0.503 $kg^{1/2}$ $mol^{-1/2}$) were calculated according to the methodology described by Moog and Voigt (2011).

The obtained complexation constant of log $*\beta^0 = -(0.06 \pm 0.24)$ at 25 °C is significantly higher than the published values in the existing literature (Table 1). The reason for the discrepancy will be debated later in the discussion part. To obtain the experimental error of the stability constant a linear regression approach of the slope analysis following the NEA guideline was used. This approach based on the corrected species distribution and includes the experimental error of the deconvolution process.

3.4. Derivation of thermodynamic data

For the determination of the molal standard enthalpy of reaction $\Delta_rH_m^0$ as well as the molal standard entropy of reaction $\Delta_rS_m^0$, a van't Hoff plot (log $*\beta^0(T)$ as a function of 1/T), based on the integrated van't Hoff equation, was used:

$$\log *\beta^0(T) = \log *\beta^0(T_0) + \frac{\Delta_r H_m^0(T_0)}{R\cdot\ln(10)}\left(\frac{1}{T_0} - \frac{1}{T}\right) \quad (5)$$

with R being the universal molar gas constant ($R = 8.314\ J \cdot K^{-1} \cdot mol^{-1}$), and T the temperature in Kelvin ($T_0 = 298.15$ K). Due to the narrow investigated temperature range (1–25 °C), the heat capacity $\Delta_rC_{p,m}^0$ was assumed to be zero and the molal enthalpy of reaction $\Delta_rH_m^0$ constant. Former studies showed that such an approximation is valid until 100 °C for complexation of actinides with inorganic and organic species (Skerencak et al., 2010; Skerencak-Frech et al., 2015). The van't Hoff plot shows a linear behavior in the observed temperature range (Fig. 5) and positive values for the molal enthalpy of reaction $\Delta_rH_m^0 = 45.8 \pm 22.5$ kJ·mol^{-1} as well as positive molal entropy of reaction $\Delta_rS_m^0 = 152.5 \pm 78.8$ J·K^{-1}·mol^{-1} were derived. The weighted linear regression and the derivation of the uncertainties on the slope and intercept at origin were performed following the NEA guideline (Lemire et al., 2013; Jordan et al., 2018).

For interactions of hard acid and bases (HSAB model, Pearson, 1968) the complexation reaction is often characterized by a positive enthalpy and entropy. The positive enthalpy term indicates that the heat required to disrupt the first hydration shell and to break the UO_2^{2+}–H_2O bond (both endothermic processes) is higher than the heat released by the bond formation between the UO_2^{2+} and $H_3SiO_4^-$

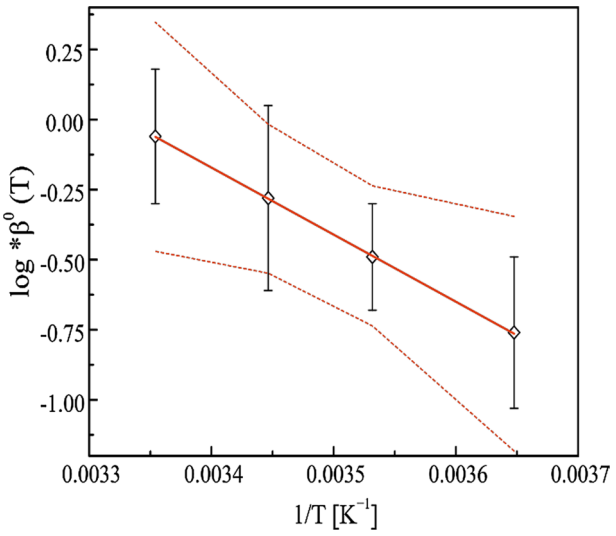

Fig. 5. Van't Hoff plot of the U(VI)-silicate complexation reaction in the temperature range between 1 and 25 °C.

molecules (exothermic process). Subsequently, the release of water from the first hydration shell to the bulk solvent will increase the disorder of the system, resulting in a positive entropy contribution. This positive reaction entropy term overcomes the unfavorable enthalpy component to promote the complex formation (Choppin and Morgenstern, 2000). Therefore, the reaction can be described as an "entropy driven" reaction. Pathak and Choppin (2006) already published a molar enthalpy and entropy of reaction for the formation of the $UO_2OSi(OH)_3^+$ complex with $\Delta_r H_m^0 = 36.3 \pm 0.9$ kJ·mol^{-1} and $\Delta_r S_m^0 = 76.0 \pm 2.7$ J·K^{-1}·mol^{-1}, respectively. As the molal enthalpy and entropy of reaction depend on the complexation constant of the reaction, this certainly explains the deviations from the values of Pathak and Choppin.

4. Discussion

Our combined ESI-MS and luminescence spectroscopic results have shown that both uranium hydrolysis and polymerization of silicate resulting in U(VI)-polysilicate complexes take place in solution depending on the experimental conditions. The obtained complexation constant at infinite dilution and at 25 °C for the $UO_2OSi(OH)_3^+$ complex in the present work log $*\beta^0 = -(0.06 \pm 0.24)$ greatly exceeds the values of any previously reported complexation constants (Table 1) by one to three orders of magnitude. Due to this large discrepancy between reported complexation constants, we will now address the possible underlying reasons for these differences.

We will begin the discussion with the hydrolysis of U(VI) and the subsequent formation of the UO_2OH^+ complex in solution. A critical review of the former studies dealing with the $UO_2OSi(OH)_3^+$ complex has shown that all authors, except Saito et al. (2015), have neglected the formation of the first uranyl(VI) hydroxo species in the acidic pH-region up to pH 4.5. Fig. SI 10 (left, open round symbols) shows a calculated species distribution between pH 0.5–5 at a uranyl(VI) concentration of $1 \cdot 10^{-5}$ M and an ionic strength of 0.2 M $NaClO_4$. Using the complexation constants recommended by the NEA TDB (Guillaumont et al., 2003), the first uranyl(VI) hydroxo species plays no role in the acidic pH-range until a pH of 4.0 (Müller et al., 2009). Drobot et al. (2016) performed luminescence spectroscopic investigations on the U(VI) hydrolysis in the trace metal concentration range (10^{-8} M), where no polynuclear species were expected. Drobot et al. (2016) determined significantly higher complexation constants for the mononuclear hydroxo species than the ones previously reported by the NEA TDB (Guillaumont et al., 2003) indicating an earlier onset of hydrolysis already at pH-values of approximately 3.0 (Fig. SI 10 left, square symbols). As we can clearly identify the presence of the 1:1 hydroxo complex UO_2OH^+ at a pH of 3.5 in the absence of aqueous silicates this complex has a great influence on the U(VI) species distribution already in the acidic range (Fig. 2). The increase of the 1:1 hydroxo complex with temperature can be explained by an increase of the complexation constant as previously observed by Kirishima et al. (2004) and Zanonato et al. (2004). Saito et al. (2015) showed the existence of a third uranyl(VI) species next to the aquo-ion and the U-Si species at pH 4 in their PARAFAC analysis of the complexation between uranyl(VI) and aqueous silicates. They attributed this species to the 1:1 U(VI) hydroxo complex. Based on these findings, it is clearly not recommendable to neglect the hydrolysis of U(VI) during the complexation studies of U(VI) with silicic acid at low pH.

Another critical point when studying the complexation between U(VI) and aqueous silicates is the solubility limit of orthosilicic acid (Fig. SI 1 in the SI). As already mentioned the solubility limit of amorphous silica in the acidic to neutral pH-range is $\approx 2 \cdot 10^{-3}$ M, with H_4SiO_4 being the main aqueous species with minor amounts of $H_3SiO_4^-$ (Iler, 1979; Sjöberg, 1996; Datnoff et al., 2001), as the the pK_a-value of silicic acid is 9.81 (Lemire et al., 2013). Therefore the formation of a 1:1 complex (log $\beta_{1:1}$) between the free uranyl UO_2^{2+} and the single deprotonate silicic acid $SiO(OH)_3^-$ is expected (see equation (2)). Above the solubility limit various oligomeric species will be formed. There are 16 reported oligomeric forms excluding the dimer $Si_2O_6H_5^-$ with up to 8 silicon atoms in the structure (Cho et al., 2006; Pelster et al., 2006). Tarutani (1989) showed by means of trimethylsilylation-gas-liquid chromatography that in a 0.01 M silicic acid solution at pH 1.8 ≈ 15 % of the silicic acid is converted to the dimer $Si_2O_7^{6-}$ and the trimer $Si_3O_{10}^{8-}$ in less than one hour. Icopini et al. (2005) also introduced an induction period in which no or less oligomerisation occurs. This period decreases with increasing oversaturation, pH, and ionic strength. Based on the literature studies presented in Table S1, only Jensen and Choppin (1998), Pathak and Choppin (2006), Saito et al. (2015) as well as Moll et al. (1998) worked in undersaturated solutions (Table 1). All other investigations were performed at oversaturation conditions with total Si concentrations exceeding up to 40 times the solubility limit of amorphous silica. Yusov and Fedoseev (2005) as well as Hrnecek and Irlweck (1999) assumed in the determination of the U(VI) complexation constant with aqueous silicates that slightly oligomerized silicic acid (dimer to tetramer) possesses the same complexation strength as monosilicic acid (Hrnecek and Irlweck, 1999; Yusov and Fedoseev, 2005). Strazhesko et al. (1974) postulated that the oligomeric silicates have a higher acidity and higher pK_a-value, which would in turn lead to the formation of stronger U-Si complexes. In the present study we demonstrated that an aqueous silicate solution of $1 \cdot 10^{-3}$ M (undersaturation conditions) at pH 3.5 and 5.0 show the presence of silicate- and Na-silicate-chains up to 7 silicon units (Fig. SI 6). These polymers form various complexes with uranyl(VI) already at moderate oversaturation conditions with $[Si]_{TOT} = 5 \cdot 10^{-3}$ M, even though their abundance in solution is much lower than that of the $UO_2OSi(OH)_3^+$ complex. More precisely, the ratio between monomeric and polymeric species in solution observed in the ESI-MS approach shifted from 16 to 5 at mild oversaturation conditions of $5 \cdot 10^{-3}$ M. In previous studies, silicon concentrations up to $8.8 \cdot 10^{-2}$ M have been used. Under such oversaturation conditions the amount of polymeric species cannot be neglected. In the ESI-MS we were able to detect U-Si polymeric species up to 4 silicate units $UO_2OSi(OH)_3(OSi(OH)_2)_3^+$. Vercouter et al. (2009) also performed ESI-MS investigations with aqueous silicates in undersaturated solutions ($1 \cdot 10^{-3}$ M) in the presence of europium. Upon increasing the pH until 5.0, they also observed the formation of oligomeric silicate species up to pentameric structures (Vercouter et al., 2009). A further increase of the uranyl(VI) concentration of $1 \cdot 10^{-4}$ M in our work showed an increase of the U-Si-species up to four Si units attached to the uranyl(VI) group. As the ESI-MS approach was performed with a lower ionic strength than the luminescence spectroscopic

approach, small differences in the amount of formed oligomeric species cannot be excluded. Marshall and Warakomski (1980) showed that 1:1 background electrolytes like NaCl or KCl only contribute to a small extent to the solubility of amorphous silica in the concentration range of 0.5 m electrolyte. However, the solubility of amorphous silica is still in the range of $2 \cdot 10^{-3}$ M. Therefore, no significant changes in the speciation of the silica monomers and oligomers are expected. Furthermore, an increase of the ionic strength to 0.2 M $NaClO_4$ in the ESI-MS samples will lead to an increased background signal due to the isotope ratio between the two chlorine isotopes ^{35}Cl and ^{37}Cl. These additional background signals will hamper the identification of relevant signals in the MS spectra. A temperature effect is not expected in the temperature range between 1 and 25 °C.

Thus, our results clearly support the fact that (i) the oligomerisation of silicic acid has to be consider already at rather low Si concentrations and (ii) the variety of possible U(VI)-polymeric Si complexes formed in oversaturated silicate solutions cannot be assumed to all exhibit the same complexation strength as the U(VI)-monosilicate species.

Both neglecting the hydrolysis and the polymerization of silicic acid will lead to an underestimation of the complexation constant of the $UO_2OSi(OH)_3^+$ complex. The polysilicates will be responsible for a reduced concentration of the $H_3SiO_4^-$ ligand in solution, while the hydrolysis of UO_2^{2+} will decrease the amount of the free uranyl(VI)-aquo ion. In the following paragraph, we will exemplarily demonstrate the influence of the latter on the magnitude of the complexation constant by using the study of Moll et al. (1998).

These authors determined the complexation constant of the $UO_2OSi(OH)_3^+$ complex using luminescence spectroscopy at 25 °C, similarly to the present study. However, the authors worked at a slightly higher pH of 3.9 (here, the pH was fixed at 3.5). A conditional complexation constant of log $*\beta = -(1.37 \pm 0.20)$ was reported, which was extrapolated to infinite dilution to obtain log $*\beta^0 = -(1.67 \pm 0.20)$. This extrapolation was later shown to be erroneous in Guillaumont et al. (2003) as well as Yusov and Fedoseev (2005), who revised the complexation constant at infinite dilution to log $*\beta^0 = -(1.11 \pm 0.20)$. We decided to re-evaluate the slope analysis of Moll et al. (1998) in the concentration range between 1.0 and $3.0 \cdot 10^{-3}$ M (Fig. 6, left). The first data point at [Si] = $1.7 \cdot 10^{-4}$ M was not taken into account, as there is a gap of one order of magnitude between this and the second data point ($1.0 \cdot 10^{-3}$ M). As the solubility limit of orthosilicic acid is $\approx 2 \cdot 10^{-3}$ M in the acid to neutral pH-range, also the last data point at $5.3 \cdot 10^{-3}$ M was omitted in the re-evaluation. The new slope analysis shows a log $*\beta$ of -0.59 with a slope close to one (1.07). This results in an extrapolated value of log $*\beta^0 = -0.32$ using the Davies equation. This complexation constant is much closer to the one reported in our study, however, it is still influenced by the hydrolysis of U(VI) which was not considered by the authors in their aqueous species distribution. Therefore, we simulated the influence of the omitted UO_2OH^+ hydrolysis species on the magnitude of the complexation constant by performing slope analysis with our spectroscopic data. For this, we added the molality of m(UO_2^{2+}) and m(UO_2OH^+), taken from our species distribution at 25 °C (Fig. 3, right), to obtain an overall "m(UO_2^{2+})" molality. The results of this simulation are shown in Fig. 6 (right). The slope of the simulation is 1.02 resulting in a conditional complexation constant of -0.56. After extrapolation to infinite dilution using the Davies equation, a value of log $*\beta^0 = -0.30$ (25 °C) was obtained. The comparison shows a good agreement between the two studies and suggests a higher complexation constant log $*\beta^0 = -(0.06 \pm 0.24)$ for the uranyl(VI)-silicate complexation than previously published. It is, furthermore, reasonable to assume that studies performed at higher pH values underestimate the complexation constant to a larger extent than studies conducted at slightly lower pH-values, as the role of hydrolysis increases with increasing pH. Fig. SI 10 (right) shows the calculated confidence interval of the species distribution based on the stability constant of $UO_2OSi(OH)_3^+$ determined in this study as well as the 1:1 hydroxo species UO_2OH^+ derived by Drobot et al. (2016). The figure clearly illustrates the broad range of existence for the U-Si and the U-OH species at pH 3.5.

Finally, we will discuss the magnitude of the complexation constant based on the effective charge of actinides. Due to the effective charge of +3.2 and +2.3 at the actinides for AnO_2^{2+} and AnO_2^+, respectively, the complexation strength follows the sequence (Choppin, 1983).

$$An^{4+} > AnO_2^{2+} > An^{3+} > AnO_2^+$$

This is clearly demonstrated for the hydrolysis, carbonate, fluoride, and phosphate complexation reaction of different trivalent and hexavalent actinides (Fig. SI 11a–d, Table SI 4) (recommended values from the NEA TDB and Nagra/PSI database (Guillaumont et al., 2003; Thoenen et al., 2014). From this it can be observed, that the complexation constants at the first complexation step with monovalent ligands (log $\beta_{1:1}$) of the hexavalent actinides are slightly higher than the complexation constants of the trivalent actinides, in agreement with the predicted complexation strength based on the effective charge. The same behavior is obtained for the An-Si complexation, when using the complexation constant obtained in the present work (see Fig. SI 11 e, Table 1, and Table SI 3). This is a further indication that the published complexation constants of the aqueous U(VI) silicate system should be re-evaluated with respect to the competing hydrolysis reaction and the solubility limit of orthosilicic acid.

5. Conclusion

In this study we could show through ESI-MS investigations that

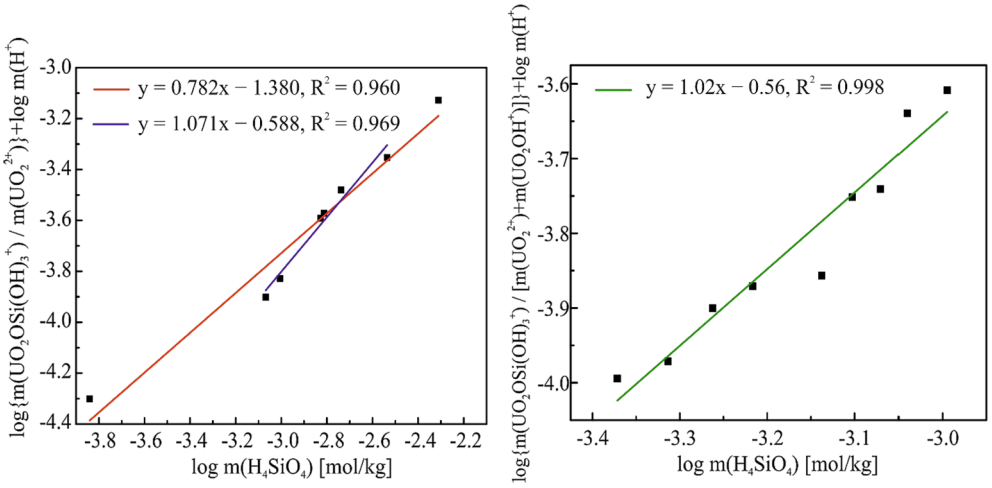

Fig. 6. Left: Re-evaluation of the slope analysis of Moll et al. (1998), disregarding the first and last data point (blue curve), raw data (red curve), at 25 °C. right: Slope analysis at 25 °C with combined m(UO_2^{2+}) + m(UO_2OH^+) to overall molality "m(UO_2^{2+})" (taken from the species distribution Fig. 3, right) as a function of log m(H_4SiO_4). (For interpretation of the references to colour in this figure legend, the reader is referred to the web version of this article.)

oligomerisation reactions of (sodium)silicate groups as well as uranyl (VI)-silicates occur already in undersaturated aqueous silicate solutions with respect to amorphous silicates. Increasing the U(VI)-concentration, the total silicate concentration, or the solution pH were found to increase the amount of aqueous U-Si and Si polymers in solution. At pH 5.0 not only the abundance of polysilicates were found to increase, but also the size of the oligomers up to 11 (sodium)silica and 4 uranyl(VI)-silica units. Irrespective of the solution conditions used in the present work, however, the prevailing solution species could be confirmed to be the monomeric $UO_2OSi(OH)_3^+$ complex. In the luminescence spectroscopic investigations, uranyl(VI) hydrolysis could be shown to occur in solution at pH 3.5 in addition to $UO_2OSi(OH)_3^+$ complex formation. The extracted complexation constant at 25 °C for the $UO_2OSi(OH)_3^+$ aqueous complex was found to be $\log {}^*\beta^0 = -(0.06 \pm 0.24)$, i.e. significantly higher than any previously reported value for this complex. The reasons for this discrepancy were attributed to the underestimation of both U(VI) hydrolysis and the formation of Si-oligomeric/colloidal species in already published studies. The hydrolysis as well as the silicate complexation will be favored with increasing temperature, which can be described by the van't Hoff equation. The positive values of the molal enthalpy (45.8 ± 22.5 kJ·mol^{-1}) and entropy (152.5 ± 78.8 J·K^{-1}·mol^{-1}) of reaction revealed an entropy-driven reaction. The obtained complexation constant indicates a higher influence of silicate ligands on the complex formation of aqueous U(VI), which may impact the mobility of U(VI) in aqueous silicate containing groundwaters.

The results of this study further indicate that a large knowledge gap for oligomeric actinide-silica species still exists. Such oligomers are likely to influence the actinide speciation under environmental conditions comprising higher silicate concentrations and circumneutral to alkaline pH-values, and should, thus, be explored in detail in future studies.

Funding

This work was supported by the German Federal Ministry of Education and Research (BMBF), Project No. 02NUK039B and 02NUK044A and the German Ministry of Economic Affairs and Energy (BMWi) 02E11334B.

CRediT authorship contribution statement

Henry Lösch: Investigation, Methodology, Validation, Formal analysis, Writing - original draft, Writing - review & editing. **Manuel Raiwa:** Investigation, Methodology, Validation. **Norbert Jordan:** Methodology, Software, Formal analysis. **Michael Steppert:** Conceptualization, Validation. **Robin Steudtner:** Methodology, Validation. **Thorsten Stumpf:** Conceptualization, Writing - original draft, Supervision. **Nina Huittinen:** Conceptualization, Validation, Writing - original draft, Writing - review & editing, Supervision, Funding acquisition.

Declaration of Competing Interest

The authors declare that they have no known competing financial interests or personal relationships that could have appeared to influence the work reported in this paper.

Appendix A. Supplementary material

Supplementary data to this article can be found online at https://doi.org/10.1016/j.envint.2019.105425.

References

Altmaier, M., Vercouter, T., 2012. Aquatic Chemistry of the Actinides: Aspects Relevant to their Environmental Behavior. Radionuclide Behaviour in the Natural Environment. Elsevier, Cambridge, pp. 44–69.
Bethke, C., 1996. Geochemical Reaction Modeling: Concepts and Applications. Oxford University Press on Demand, New York.
Brasser, T., Droste, J., Müller-Lyda, I., Neles, J., Sailer, M., Schmidt, G., Steinhoff, M., 2008. Endlagerung wärmeentwickelnder radioaktiver Abfälle in Deutschland, Braunschweig/Darmstadt, GRS-247 Hauptband.
Bruno, J., Ewing, R.C., 2006. Spent nuclear fuel. Elements 2, 343–349.
Burrows, H.D., 1990. Electron transfer from halide ions to uranyl (2+) excited-state ions in aqueous solution: formation and decay of dihalide radical anions. Inorg. Chem. 29, 1549–1554.
Cho, H., Felmy, A.R., Craciun, R., Keenum, J.P., Shah, N., Dixon, D.A., 2006. Solution state structure determination of silicate oligomers by ^{29}Si-NMR spectroscopy and molecular modeling. J. Am. Chem. Soc. 128, 2324–2335.
Choppin, G., Liljenzin, J.-O., Rydberg, J., 2013. Radiochemistry and nuclear chemistry, Amsterdam, 4 ed. Butterworth-Heinemann, pp. 514–786.
Choppin, G.R., 1983. Solution Chemistry of the Actinides. Radiochim. Acta 32, 43–54.
Choppin, G.R., Morgenstern, A., 2000. Thermodynamics of solvent extraction. Solvent Extr. Ion Exch. 18, 1029–1049.
Datnoff, L.E., Snyder, G.H., Korndörfer, G.H., 2001. Silicon in Agriculture. Elsevier, Amsterdam, pp. 57–85.
Drobot, B., Bauer, A., Steudtner, R., Tsushima, S., Bok, F., Patzschke, M., Raff, J., Brendler, V., 2016. Speciation studies of metals in trace concentrations: the mononuclear uranyl(VI) hydroxo complexes. Anal. Chem. 88, 3548–3555.
Fanghänel, T., Weger, H., Könnecke, T., Neck, V., Paviet-Hartmann, P., Steinle, E., Kim, J., 1998. Thermodynamics of Cm (III) in concentrated electrolyte solutions. Carbonate complexation at constant ionic strength (1 m NaCl). Radiochim. Acta 82, 47–54.
Gibb, F.G., 1999. High-temperature, very deep, geological disposal: a safer alternative for high-level radioactive waste? Waste Manage. 19, 207–211.
Giffaut, E., Grivé, M., Blanc, P., Vieillard, P., Colàs, E., Gailhanou, H., Gaboreau, S., Marty, N., Made, B., Duro, L., 2014. Andra thermodynamic database for performance assessment: ThermoChimie. Appl. Geochem. 49, 225–236.
Grambow, B., 2006. Nuclear waste glasses-How durable? Elements 2, 357–364.
Guillaumont, R., Fanghänel, T., Neck, V., Fuger, J., Palmer, D., Grenthe, I., Rand, M., 2003. Update on the Chemical Thermodynamics of Uranium, Neptunium, Plutonium, Americium and Technetium, Chemical Thermodynamics 5, Issy-les-Moulineaux. Nuclear Energy Agency, Elsevier Science Publisher.
Haubitz, T., Tsushima, S., Steudtner, R., Drobot, B., Geipel, G., Stumpf, T., Kumke, M.U., 2018. Ultrafast Transient Absorption Spectroscopy of UO_2^{2+} and $[UO_2Cl]^+$. J. Phys. Chem. A 122, 6970–6977.
Hedin, A., 1997. Spent nuclear fuel-how dangerous is it? A report from the project'Description of risk', Stockholm, Swedish Nuclear Fuel and Waste Management Co.
Hrnecek, E., Irlweck, K., 1999. Formation of Uranium(VI) Complexes with Monomeric and Polymeric Species of Silicic Acid. Radiochim. Acta 87, 29–35.
Huittinen, N., Rabung, T., Schnurr, A., Hakanen, M., Lehto, J., Geckeis, H., 2012. New insight into Cm (III) interaction with kaolinite–Influence of mineral dissolution. Geochim. Cosmochim. Acta 99, 100–109.
Icopini, G.A., Brantley, S.L., Heaney, P.J., 2005. Kinetics of silica oligomerization and nanocolloid formation as a function of pH and ionic strength at 25 °C. Geochim. Cosmochim. Acta 69, 293–303.
Iler, K.R., 1979. The chemistry of silica: Solubility, Polymerization, Colloid and Surface Properties and Biochemistry of Silica. John Wiley and Sons, New York.
Jensen, M.P., Choppin, G.R., 1998. Complexation of Uranyl(VI) by Aqueous Orthosilicic Acid. Radiochim. Acta 82, 83–88.
Jordan, N., Demnitz, M., Lösch, H., Starke, S., Brendler, V., Huittinen, N., 2018. Complexation of Trivalent Lanthanides (Eu) and Actinides (Cm) with Aqueous Phosphates at Elevated Temperatures. Inorg. Chem. 57, 7015–7024.
Kim, J.-S., Kwon, S.-K., Sanchez, M., Cho, G.-C., 2011. Geological storage of high level nuclear waste. KSCE J. Civ. Eng. 15, 721–737.
Kirishima, A., Kimura, T., Tochiyama, O., Yoshida, Z., 2004. Speciation study on uranium (VI) hydrolysis at high temperatures and pressures. J. Alloys Compd. 374, 277–282.
Grenthe, I., Drożdżyński, J., Fujino, T., Buck, E.C., Albrecht-Schmitt, T.E., Wolf, S.F., 2006. Uranium. In: Morss, L.R., Edelstein, N.M., Fuger, J., Katz, J.J. (Eds.), The Chemistry of the Actinide and Transactinide Elements (Volume 1), third ed. Springer, Dordrecht, pp. 302–317.
Lemire, R.J., Berner, U., Musikas, C., Palmer, D.A., Taylor, P., Tochiyama, O., Perrone, J., 2013. Chemical thermodynamics of iron-Part 1-Chemical thermodynamics volume 13a, Issy-les-Moulineaux, Nuclear Energy Agency.
Maher, K., Bargar, J.R., Brown Jr, G.E., 2012. Environmental Speciation of Actinides. Inorg. Chem. 52, 3510–3532.
Marshall, W.L., 1980. Amorphous silica solubilities—I. Behavior in aqueous sodium nitrate solutions; 25–300 °C, 0–6 molal. Geochim. Cosmochim. Acta 44, 907–913.
Marshall, W.L., Warakomski, J.M., 1980. Amorphous silica solubilities—II. Effect of aqueous salt solutions at 25 °C. Geochim. Cosmochim. Acta 44, 915919–917924.
Moll, H., Geipel, G., Brendler, V., Bernhard, G., Nitsche, H., 1998. Interaction of uranium (VI) with silicic acid in aqueous solutions studied by time-resolved laser-induced fluorescence spectroscopy (TRLFS). J. Alloys Compd. 271–273, 765–768.
Moog, H.C., Voigt, W., 2011. Thermodynamic Reference Database. Dielectric Constant, Vapor Pressure, and Density of Water and the Calculation of Debye-Hückel Parameters ADH, BDH, and Aφ for Water. THEREDA Technical Paper.
Moulin, C., 2003. On the use of time-resolved laser-induced fluorescence (TRLIF) and electrospray mass spectrometry (ES-MS) for speciation studies. Radiochim. Acta 91, 651–658.
Moulin, C., Charron, N., Plancque, G., Virelizier, H., 2000. Speciation of uranium by

electrospray ionization mass spectrometry: Comparison with time-resolved laser-induced fluorescence. Appl. Spectrosc. 54, 843–848.
Moulin, C., Decambox, P., Moulin, V., Decaillon, J.G., 1995. Uranium speciation in solution by time-resolved laser-induced fluorescence. Anal. Chem. 67, 348–353.
Moulin, C., Laszak, I., Moulin, V., Tondre, C., 1998. Time-resolved laser-induced fluorescence as a unique tool for low-level uranium speciation. Appl. Spectrosc. 52, 528–535.
Müller, K., Foerstendorf, H., Tsushima, S., Brendler, V., Bernhard, G., 2009. Direct spectroscopic characterization of aqueous actinyl (VI) species: a comparative study of Np and U. J. Phys. Chem. A 113, 6626–6632.
Myllykylae, E., 2008-2009. Reduction of uranium in disposal conditions of spent nuclear fuel, Olkiluoto, POSIVA-WR–08-09.
OECD/NEA, 2006. The Economics of the Back End of the Nuclear Fuel Cycle, Paris, Organisation for Economic Co-operation and Development/Nuclear Energy Agency (OECD/NEA).
Parkhurst, D.L., Appelo, C., 1999. User's guide to PHREEQC (Version 2): A computer program for speciation, batch-reaction, one-dimensional transport, and inverse geochemical calculations, Denver, U.S. DEPARTMENT OF THE INTERIOR; U.S. GEOLOGICAL SURVEY.
Pathak, P., Choppin, G.R., 2006. Thermodynamic study of metal silicate complexation in perchlorate media. Radiochim. Acta 94, 81–86.
Pearson, R.G., 1968. Hard and soft acids and bases, HSAB, part 1: Fundamental principles. J. Chem. Educ. 45, 581.
Pelster, S.A., Schrader, W., Schüth, F., 2006. Monitoring temporal evolution of silicate species during hydrolysis and condensation of silicates using mass spectrometry. J. Am. Chem. Soc. 128, 4310–4317.
Porter, R.A., Weber, W.J., 1971. The interaction of silicic acid with iron(III) and uranyl ions in dilute aqueous solution. J. Inorg. Nucl. Chem. 33, 2443–2449.
Reiller, P.E., Vercouter, T., Duro, L., Ekberg, C., 2012. Thermodynamic data provided through the FUNMIG project: Analyses and prospective. Appl. Geochem. 27, 414–426.
Saito, T., Aoyagi, N., Kimura, T., 2015. Time-resolved laser-induced fluorescence spectroscopy combined with parallel factor analysis: a robust speciation technique for UO_2^{2+}. J. Radioanal. Nucl. Chem. 303, 1129–1132.
Satoh, I., Choppin, G., 1992. Interaction of Uranyl(VI) with Silicic Acid. Radiochim. Acta 56, 85–88.
Schröder, D., 2012. Ion clustering in electrospray mass spectrometry of brine and other electrolyte solutions. Phys. Chem. Chem. Phys. 14, 6382–6390.
Siever, R., 1957. The silica budget in the sedimentary cycle. Am. Mineral. 42, 821–841.
Sjöberg, S., 1996. Silica in aqueous environments. J. Non-Cryst. Solids 196, 51–57.
Skerencak-Frech, A., Maiwald, M., Trumm, M., Froehlich, D.R., Panak, P.J., 2015. The Complexation of Cm (III) with Oxalate in Aqueous Solution at T = 20–90 °C: A Combined TRLFS and Quantum Chemical Study. Inorg. Chem. 54, 1860–1868.
Skerencak, A., Panak, P.J., Neck, V., Trumm, M., Schimmelpfennig, B., Lindqvist-Reis, P., Klenze, R., Fanghänel, T., 2010. Complexation of Cm (III) with Fluoride in Aqueous Solution in the Temperature Range from 20 to 90 °C. A Joint TRLFS and Quantum Chemical Study. J. Phys. Chem. B 114, 15626–15634.
Söhnel, O., Novotny, P., 1985. Densities of Aqueous Solutions of Inorganic Substances. Elsevier, Amsterdam.
Strazhesko, D.N., Strelko, V.B., Belyakov, V.N., Rubanik, S.C., 1974. Mechanism of cation exchange on silica gels. J. Chromatogr. A 102, 191–195.
Tarutani, T., 1989. Polymerization of Silicic Acid A Review. Anal. Sci. 5, 245–252.
Thoenen, T., Hummel, W., Berner, U., Curti, E., 2014. The PSI/Nagra Chemical Thermodynamic Database 12/07, Villigen, PSI.
Tsushima, S., Götz, C., Fahmy, K., 2010. Photoluminescence of uranium (VI): quenching mechanism and role of uranium (V). Chemistry–A. Eur. J. 16, 8029–8033.
Vercouter, T., Casanova, F., Calvo, A., Amekraz, B., Moulin, C., 2009. 4th annual workshop proceedings of the integrated project “fundamental processes of radionuclide migration. In: Buckau, G., Duro, L., Kienzler, B., MontoyaandA, V. (Eds.), 6th EC FP IP FUNMIG) 24. - 27. November 2008. Delos. Karlsruhe, pp. 263–270.
Yokoyama, Y., Moriyasu, M., Ikeda, S., 1976. Electron transfer mechanism in quenching of uranyl luminescence by halide ions. J. Inorg. Nucl. Chem. 38, 1329–1333.
Yusov, A., Fedoseev, A., 2003. Reaction of Plutonium(VI) with Orthosilicic Acid $Si(OH)_4$. Russ. J. Coord. Chem. 29, 582–590.
Yusov, A., Fedoseev, A., 2005. A spectrophotometric study of the interaction of uranyl ions with orthosilicic acid and polymeric silicic acids in aqueous solutions. Radiochemistry 47, 345–351.
Yusov, A., Shilov, V., Fedoseev, A., Astafurova, L., Delegard, C.H., 2005. A spectrophotometric study of the interaction of Np(VI) with orthosilicic acid and polymeric silicic acids in aqueous solutions. Radiochemistry 47, 352–357.
Zanonato, P., Di Bernardo, P., Bismondo, A., Liu, G., Chen, X., Rao, L., 2004. Hydrolysis of Uranium(VI) at variable temperatures (10–85 °C). J. Am. Chem. Soc. 126, 5515–5522.
Zubarev, R.A., Makarov, A., 2013. Orbitrap mass spectrometry. Anal. Chem. 85, 5288–5296.